



ChemComm

**Melamine-Induced Synthesis of a Structurally Perfect  
Kagomé Antiferromagnet**

Journal:	<i>ChemComm</i>
Manuscript ID	CC-COM-01-2022-000416.R1
Article Type:	Communication

SCHOLARONE™  
Manuscripts

## ARTICLE

## Melamine-Induced Synthesis of a Structurally Perfect Kagomé Antiferromagnet

Yongbing Shen<sup>\*a</sup>, Kunihisa Sugimoto<sup>b</sup>, Satoshi Yamashita<sup>c</sup>, Takefumi Yoshida<sup>d</sup>, Yasuhiro Nakazawa<sup>c</sup>, Brian K. Breedlove<sup>a</sup>, Haitao Zhang<sup>e</sup> and Masahiro Yamashita<sup>\*a,f</sup>

Received 00th January 20xx,  
Accepted 00th January 20xx

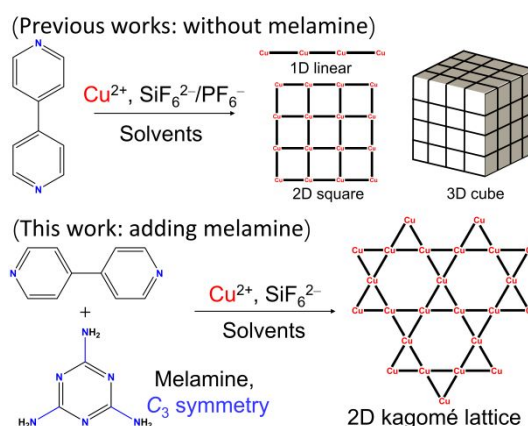
DOI: 10.1039/x0xx00000x

We report here a structurally perfect kagomé lattice  $\{[\text{Cu}_3(\text{bpy})_6](\text{SiF}_6)_3(\text{melamine})_3\}_n$  (**1**), where bpy is 4,4'-bipyridine and  $[\text{SiF}_6]^{2-}$  is hexafluorosilicate anion. In comparison to general 1D linear, 2D layered and 3D cubic metal-organic frameworks, by using  $\text{Cu}^{2+}$  nodes and bpy ligands, a perfect kagomé lattice was synthesized by introducing  $C_3$  symmetrical melamine molecules. Magnetic susceptibility and low-temperature heat capacity measurements indicated weak antiferromagnetic interactions between the spins and no long-range magnetic ordering to 0.7 K. Using  $C_3$  symmetrical melamine molecules can be considered as a challenging synthetic strategy to afford new topological materials.

Two-dimensional metal-organic frameworks (2D MOFs) hold promise as models for exploring exotic quantum phenomena, such as conductivity and quantum-spin liquids (QSLs)<sup>1</sup>. The structures widely recognized as exhibiting QSL behaviours are 2D kagomé lattices because of their high degree of charge localization, which is crucial for understanding the mechanism of QSL state<sup>2</sup>. In the past decades, natural mineral  $\text{Cu}^{2+}$ -based antiferromagnetic kagomé compounds, such as volborthite<sup>3</sup>, herbertsmithite<sup>4</sup> and vesignieite<sup>5</sup>, have been regarded as the candidates for QSLs. These compounds exhibit 2D features, of which the kagomé layers are separated by the nonmagnetic oxides and solvents, yielding layered kagomé lattices. Nevertheless, a small amount of fractional magnetic  $\text{Cu}^{2+}$  impurities are present in the nonmagnetic layers, breaking the magnetic two-dimensionality. Recently, K. Awaga et al. have used  $\text{Cu}^{2+}$  nodes and a  $C_3$  symmetric hexahydroxytriphenylene (HHTP) ligand to produce a weak kagomé antiferromagnet,  $\text{Cu}_3(\text{HHTP})_2$ . From heat capacity measurement, there is no magnetic ordering to 0.03 K<sup>6</sup>. However, the potential  $\pi$ - $\pi$  interactions in the layers could interfere with the pure 2D kagomé magnetism. Meanwhile, N. Jiang et al. have reported a  $d^1$ -titanium ( $\text{Ti}^{3+}$ ) fluoride kagomé compound,  $(\text{CH}_3\text{NH}_3)_2\text{NaTiF}_{12}$ . By changing the magnetic interaction pathway, a

perfect  $S = \frac{1}{2}$  kagomé antiferromagnet with no long-range magnetic ordering to 0.1 K was identified<sup>1d</sup>.

### Scheme 1. Synthesis of Cu(bpy)-based MOFs with/without adding melamine.



Although 2D kagomé compounds show interesting quantum phenomena, it is still difficult to systematically synthesize structurally perfect kagomé lattices. Therefore, exploring new synthetic strategies is necessary. Thus, we selected bipyridine as a ligand to synthesize a perfect kagomé compound by adding a symmetrical molecule. The bipyridine was chosen because it was shown to mediate the electronic effects between two paramagnetic centers<sup>7</sup> and because it could be used to prepare various architectures, including 1D linear, 2D square, and 3D cubic MOFs<sup>8</sup> (Scheme 1). Interestingly, we found that the above-mentioned architectures can be structurally tuned by the addition of some symmetric molecules during the synthesis. Herein, we report a structurally perfect 2D kagomé lattice based on the  $\text{Cu}(\text{bpy})_2(\text{SiF}_6)$  system, which has not been observed so far. By using  $C_3$  symmetrical melamine molecules, solvothermal synthesis produced hexagonal prism-like crystals,

<sup>a</sup> Department of Chemistry, Graduate School of Science, Tohoku University, 6-3 Aramaki-Aza-Aoba, Aoba-Ku, Sendai 980-8578, Japan. shen.yongbing.b1@tohoku.ac.jp

<sup>b</sup> Diffraction & Scattering Division, Japan Synchrotron Radiation Research Institute (ASRI), 1-1-1 Kouto, Sayo-Cho, Sayo-Gun, Hyogo 679-5198, Japan.

<sup>c</sup> Department of Chemistry, Graduate School of Science, Osaka University, Toyonaka, Osaka 560-0043, Japan.

<sup>d</sup> Innovation Research Center for Fuel Cells, The University of Electro-Communications, Chofu, Tokyo 182-8585, Japan

<sup>e</sup> Institute of Inorganic and Applied Chemistry, University of Hamburg, Martin-Luther-King-Platz 6, 20146 Hamburg, Germany

<sup>f</sup> School of Materials Science and Engineering, Nankai University, Tianjin 300350, China.

Electronic Supplementary Information (ESI) available: Experimental details and supporting figures. CCDC NO: 2089538, 2100380-2100385. See DOI: 10.1039/x0xx00000x

## ARTICLE

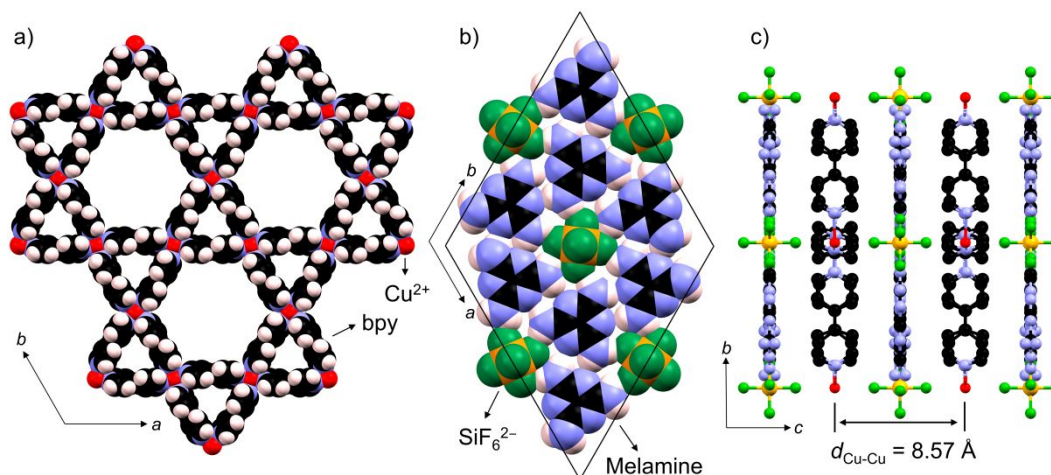


**Figure 1.** Crystal structure at 300 K. (a) The structure of the kagomé layer with all Cu<sup>2+</sup> ions coordinated by four bpy ligands crystallized in one plane. (b) The structure of the counter anion layer. Some short contacts (N-H...F) were observed between melamine and [SiF<sub>6</sub>]<sup>2-</sup> ions. Meanwhile, (N-H...N) hydrogen bonds between the melamine were observed. (c) Crystal packing in the *bc* plane.

whereas cubic crystals formed when melamine was not used in the previous works. From synchrotron X-ray ( $\lambda = 0.4132 \text{ \AA}$ ) structure analysis, compound **1** crystallized in the hexagonal space group *P6/mcc* with the following cell parameters:  $a = b = 22.03(2) \text{ \AA}$ ,  $c = 17.14(3) \text{ \AA}$  and  $\beta = 120^\circ$  at 300 K (Table S1). The single-crystal morphology was a well-shaped hexagon-like prism with a typical size (length  $\times$  width  $\times$  height  $\approx 40 \times 40 \times 30 \text{ \mu m}^3$ ) (Figure S1). The X-ray diffraction patterns indicated that the solvothermal method produced high-quality single-crystals (Figure S2). In the *ab* plane, Cu<sup>2+</sup>-based trihexagonal tiling patterns, consisting of equilateral triangles and regular hexagons, were observed (Figure 1a). This structural arrangement is called a kagomé pattern. The equilateral triangles contained three bpy molecules and three Cu<sup>2+</sup> ions with Cu–N bond lengths of 2.03 Å and  $\angle \text{N–Cu–N}$  of 86.46° and 93.65°. The coordination geometry around the Cu<sup>2+</sup> ions is nearly square planar with *D<sub>4h</sub>* symmetry. The Cu...Cu distance between adjacent triangles was determined to be 11.0 Å. In the [SiF<sub>6</sub>]<sup>2-</sup> layer, one central dianion [SiF<sub>6</sub>]<sup>2-</sup> was surrounded by six melamine molecules via N–H...F interactions (Figure 1b). The resulting hexagonal pattern of melamine molecules interacted with each other via N–H...N hydrogen bonds. In addition, along the *c* axis, the bpy ligands interacted with melamine molecules via C–H...N contacts (Figure S3). In other words, it appears that melamine molecules played an important role in the formation of the kagomé lattice. The long-distance (2.509 Å) between Cu<sup>2+</sup> and F<sup>-</sup> ions along the *c* axis indicates that there are weak van der Waals' forces between the kagomé and counter anion layers (Figure S4). Therefore, the separation between the two adjacent kagomé layers (8.57 Å) efficiently minimizes the interlayer

spin interactions (Figure 1c). To determine the phase purities of the crystal structures, temperature-dependence of single-crystal X-ray diffractions were performed in the additional 200, 100, 80, 50 and 20 K. The unit-cell parameters remained consistent in 20–300 K (Table S2). The structural analysis clearly showed the presence of disordered melamine molecules to 20 K. The powder X-ray diffraction (PXRD) patterns indicated that there are no structural changes in 20–300 K (Figure 2).

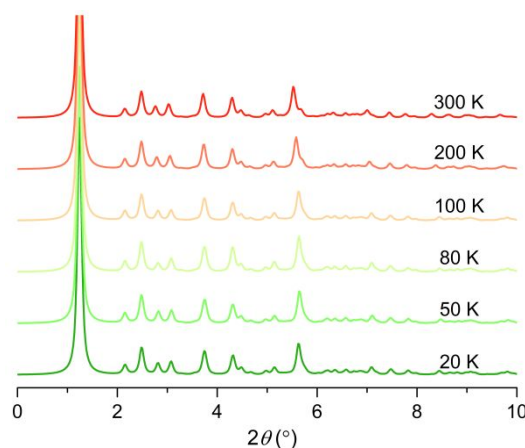


**Figure 2.** The PRXD patterns at various temperatures.

M. Verdaguer et al. have shown that the larger the nonorthogonal magnetic orbitals, the stronger the antiferromagnetic exchange interactions between metallic centres are.<sup>9</sup> Antiferromagnetic coupling between two Cu<sup>2+</sup>  $d_{x^2-y^2}$  orbitals through the bpy ligands

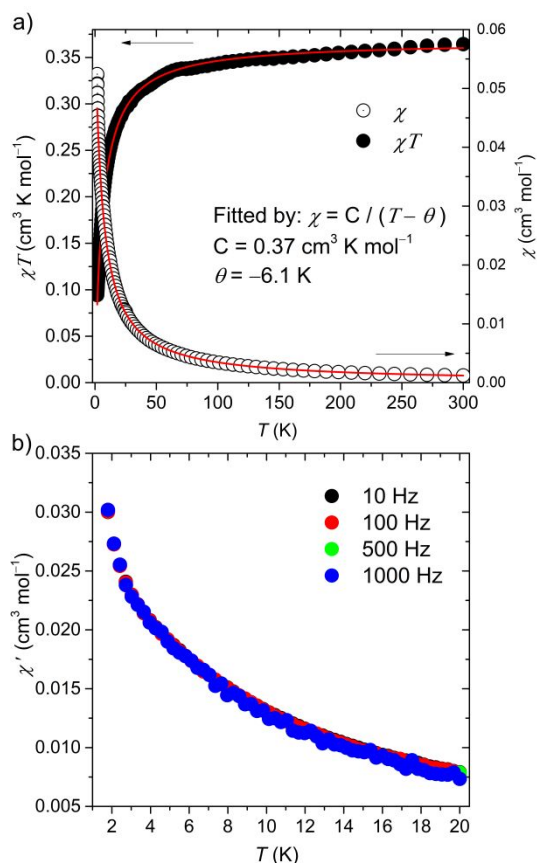


**Figure 3.** (a) Temperature dependence of the magnetic susceptibility ( $\chi$ ) and  $\chi T$  in the temperature range of 1.8–300 K. The data were fitted by using Curie-Weiss law. (b) Temperature dependence of real part of alternating current magnetic susceptibility ( $\chi'$ ) in the temperature range of 1.8–20 K in various frequencies.

in a dinuclear system have been reported by M. Julve et al.<sup>10</sup>. Therefore, we predicted that **1** would adopt an antiferromagnetic ground state in the kagomé lattice. Temperature-dependent magnetic susceptibility data ( $\chi$ - $T$ , Figure 3a) in a 1000 Oe field indicated paramagnetic-like behaviour in the temperature range of 1.8–300 K. Fitting the data with the Curie-Weiss equation afforded a negative Curie-Weiss temperature ( $\theta_{\text{CW}}$ ) of -6.1 K (Figure S5), indicating that there is weak antiferromagnetic exchange coupling between the  $\text{Cu}^{2+}$  spin centres. The exchange coupling parameter  $J$  between adjacent spin centres was calculated for molecular solids with a molecular field solution by using the equation  $\theta_{\text{CW}} = zJ$ , where  $z$  is the number of neighbours.  $J = -1.6 \text{ cm}^{-1}$ , obtained with  $z$  fixed at 4, and this value is similar to that for a dinuclear  $\text{Cu}_2(\text{bpy})$  metal complex ( $J = -0.7 \text{ cm}^{-1}$ )<sup>10</sup>. In addition, the low-temperature (1.8–20 K) real part of alternating current (*ac*) susceptibilities ( $\chi'$ ) at various frequencies in zero field indicated that there was no magnetic ordering (Figure 3b)<sup>1d</sup>. L. Noodleman has proposed a theoretic model for low-spin states to estimate the  $J$  from broken-symmetry wavefunction<sup>11</sup>. The broken symmetry state is an equal mixture of the lowest and highest spin states, which is strictly valid only for broken symmetry determinants with two  $S = \frac{1}{2}$  centres in the weak overlap limit. We calculated the intralayer  $J'$  and interlayer  $J''$  by using

density-function theory (DFT) B3LYP/def2TZVP basis set in two different structure models (Figure S6). The calculated intralayer  $J'(-1.1 \text{ cm}^{-1})$  shows a comparable value to the experimental  $J$ . Meanwhile,  $J'$  is greater than the interlayer  $J''(0.017 \text{ cm}^{-1})$ , indicating compound **1** is a 2D magnetic MOF.

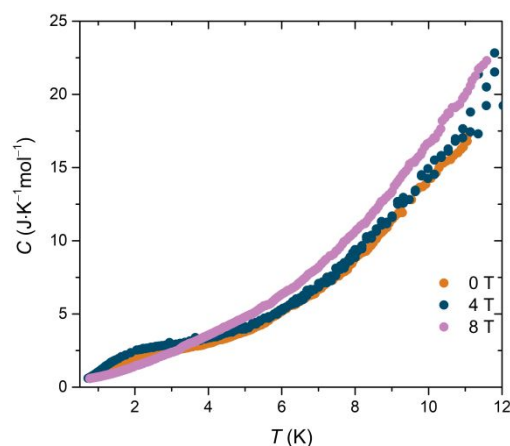


**Figure 4.** Temperature dependence of the total heat capacity in the  $T$  range of 0.7–12 K in several applied magnetic fields.

Like magnetic susceptibilities, heat capacities are useful for unearthing hidden magnetic phase transitions<sup>2,6</sup>. The total low-temperature heat capacity,  $C$ , which includes both the magnetic and lattice contributions, were measured in 0, 4, 8 T magnetic fields (Figure 4). There were no sharp peaks in the range of 0.7–12 K, indicating the absence of long-range magnetic order in this temperature range<sup>1d,6,12</sup>. In other words, the combination of low-temperature heat capacities and magnetic susceptibilities provide evidence for the absence of long-range magnetic ordering to 0.7 K. The frustration parameter<sup>2</sup>  $f$  is defined as the absolute ratio of the Weiss temperature,  $\Theta_{\text{CW}}$ , over the Neel temperature,  $T_{\text{N}}$  ( $f = |\Theta_{\text{CW}}|/T_{\text{N}}$ ) is greater than 8.9, indicating strong suppression of the magnetic ordering.

In summary, we demonstrated how a structurally perfect kagomé lattice based on the  $\text{Cu}(\text{bpy})_2(\text{SiF}_6)$  system was synthesized by using  $C_3$  symmetrical melamine molecules. The low temperature magnetic and heat capacity measurements indicated that **1** had a mild magnetic frustrated ground state above 0.7 K. Compared to inorganic kagomé compounds, organic-inorganic hybrids such as MOFs potentially allow for a readily fine-tuning of parameters to manipulate the electronic properties. Adding such symmetrical molecules could be a challenging strategy for preparing new topological materials.

This work was partially supported by CREST, JST Grant Number JPMJCR12L3. M.Y thanks for the support from the 111 Project (B18030) from China. Y. S thanks for the valuable discussion with Dr Hiroaki Iguchi for crystal structure analysis.

## Conflicts of interest

There are no conflicts to declare.

## References

- 1 (a) Zhang, B.; Zhang, Y.; Wang, Z. M.; Wang, D. W.; Baker, P. J.; Pratt, F. L.; Zhu, D. B. *Sci. Rep.* 2014, **4**, 6451; (b) Chen, S.; Dai, J.; Zeng, X. C. *Phys. Chem. Chem. Phys.* 2015, **17** (8), 5954-5958; (c) Huang, X.; Zhang, S.; Liu, L. Y.; Yu, L.; Chen, G. F.; Xu, W.; Zhu, D. B. *Angew. Chem. Int. Ed.* 2018, **57** (1), 146-150; (d) Jiang, N. X.; Ramanathan, A.; Bacsa, J.; La Pierre, H. S. *Nat. Chem.* 2020, **12** (8), 691-696; (e) Takenaka, T.; Ishihara, K.; Roppongi, M.; Miao, Y.; Mizukami, Y.; Makita, T.; Tsurumi, J.; Watanabe, S.; Takeya, J.; Yamashita, M.; Torizuka, K.; Uwatoko, Y.; Sasaki, T.; Huang, X.; Xu, W.; Zhu, D.; Su, N.; Cheng, J. G.; Shibauchi, T.; Hashimoto, K. *Sci. Adv.* 2021, **7** (12), eabf3996; (f) Chakraborty, G.; Park, I. H.; Medishetty, R.; Vittal, J. J. *Chem. Rev.* 2021, **121** (7), 3751-3891.
- 2 Balents, L. *Nature* 2010, **464** (7286), 199-208.
- 3 (a) Hiroi, Z.; Hanawa, M.; Kobayashi, N.; Nohara, M.; Takagi, H.; Kato, Y.; Takigawa, M. *J. Phys. Soc. Jpn.* 2001, **70** (11), 3377-3384; (b) Yoshida, M.; Takigawa, M.; Yoshida, H.; Okamoto, Y.; Hiroi, Z. *Phys. Rev. Lett.* 2009, **103** (7), 077207.
- 4 (a) Shores, M. P.; Nytko, E. A.; Bartlett, B. M.; Nocera, D. G., A structurally perfect  $S = 1/2$  kagome antiferromagnet. *J. Am. Chem. Soc.* 2005, **127** (39), 13462-13463; (b) Norman, M. R. *Rev. Mod. Phys.* 2016, **88** (4), 041002.
- 5 (a) Okamoto, Y.; Yoshida, H.; Hiroi, Z. *J. Phys. Soc. Jpn.* 2009, **78** (3), 033701; (b) Boldrin, D.; Fak, B.; Canevet, E.; Ollivier, J.; Walker, H. C.; Manuel, P.; Khalyavin, D. D.; Wills, A. S. *Phys. Rev. Lett.* 2018, **121** (10), 107203; (c) Boldrin, D.; Knight, K.; Wills, A. S. *J. Mater. Chem. C* 2016, **4** (43), 10315-10322.
- 6 Misumi, Y.; Yamaguchi, A.; Zhang, Z. Y.; Matsushita, T.; Wada, N.; Tsuchiizu, M.; Awaga, K. *J. Am. Chem. Soc.* 2020, **142** (39), 16513-16517.
- 7 (a) Zeng, M. H.; Zhang, W. X.; Sun, X. Z.; Chen, X. M. *Angew. Chem. Int. Ed.* 2005, **44** (20), 3079-3082; (b) Chen, Z.; Gao, D. L.; Diao, C. H.; Liu, Y.; Ren, J.; Chen, J.; Zhao, B.; Shi, W.; Cheng, P. *Cryst. Growth. Des.* 2012, **12** (3), 1201-1211; (c) Manson, J. L.; Lecher, J. G.; Gu, J. Y.; Geiser, U.; Schlueter, J. A.; Henning, R.; Wang, X. P.; Schultz, A. J.; Koo, H. J.; Whangbo, M. H. *Dalton. T.* 2003, **14**, 2905-2911.
- 8 (a) Noro, S.; Kitaura, R.; Kondo, M.; Kitagawa, S.; Ishii, T.; Matsu-zaka, H.; Yamashita, M. *J. Am. Chem. Soc.* 2002, **124** (11), 2568-2583; (b) Lu, J. Y.; Cabrera, B. R.; Wang, R. J.; Li, J. *Inorg. Chem.* 1999, **38** (20), 4608-4611.
- 9 Verdaguer, M.; Kahn, O.; Julve, M.; Gleizes, A. *Nouv. J. Chim.* 1985, **9** (5), 325-334.
- 10 Jule, M.; Verdaguer, M.; Faus, J.; Tinti, F.; Moratal, J.; Monge, A.; Gutierrezpuebla, E. *Inorg. Chem.* 1987, **26** (21), 3520-3527.
- 11 Noodleman J. *J. Chem. Phys.* 1981, **74**, 5737.
- 12 (a) Yoshida, H. K.; Noguchi, N.; Ishii, Y.; Oda, M.; Chen, J.; Yamaura, K.; Yamashita, S.; Nakazawa, Y.; Kida, T.; Narumi, Y.; Hagiwara, M. *J. Phys. Soc. Jpn.* 2021, **90** (4), 044714; (b) Yamashita, S.; Moriura, T.;

Nakazawa, Y.; Yoshida, H.; Okamoto, Y.; Hiroi, Z. *J. Phys. Soc. Jpn.* 2010, **79** (8), 083710.